# Adaptive Modularity for Power Electronics Based Electrolysis Systems for Green Hydrogen

Deshmukh, Rohan Shailesh ; Shekhar, Aditya; Bauer, Pavol

**DOI**
10.1109/PEMC51159.2022.9962941

**Publication date**
2022

**Document Version**
Final published version

**Published in**
Proceedings of the 2022 IEEE 20th International Power Electronics and Motion Control Conference (PEMC)

# Adaptive Modularity for Power Electronics Based Electrolysis Systems for Green Hydrogen

Rohan Shailesh Deshmukh
*dept. Electrical Sustainable Energy*
*Delft University of Technology*
Delft, The Netherlands
r.s.deshmukh@tudelft.nl

Aditya Shekhar
*dept. Electrical Sustainable Energy*
*Delft University of Technology*
Delft, The Netherlands
A.Shekhar@tudelft.nl

Pavol Bauer
*dept. Electrical Sustainable Energy*
*Delft University of Technology*
Delft, The Netherlands
P.Bauer@tudelft.nl

2022 IEEE 20th International Power Electronics and Motion Control Conference (PEMC) | 978-1-6654-9681-0/22/$31.00 ©2022 IEEE | DOI: 10.1109/PEMC51159.2022.9962941

***Abstract*—Electrolysis holds tremendous potential in reducing the carbon footprint and providing energy dense fuels such as methane. Such systems can be integrated with renewable energy systems with the aid of power electronics interfaces. However, this integration is not straight-forward and imposes various converter design challenges. This paper presents the current state-of-the-art electrolyzer systems, and a simple model of an alkaline regenerative stack with four degrees of freedom. To gain insights with regards to limitations/trade-offs, a sensitivity analysis is conducted on this model. Based on these insights, the challenges associated with power electronics converter design for this application have been discussed along with the trade-offs associated with the electrolyser system. Furthermore, the concept of adaptive modularity for efficiency and reliability improvement has been discussed.**

***Index Terms*—Power electronics, electrolysis, modelling, sensitivity analysis, modularity and reconfigurability in power electronic systems, isolated converter topologies, green hydrogen.**

## I. Introduction

The emissions of greenhouse gases especially $CO_2$ have increased drastically over a few years. As a result, there has been a collective effort to reduce these emissions with the emphasis on diminishing their detrimental impacts on the climate including the increase in average global temperature.

In the Netherlands, the Klimaatakkoord aims at the reduction of $CO_2$ emissions by 49% in 2030 and 95% in 2050 relative to the 1990 levels [1]. This is well aligned with the targets set by the European Union (EU) with regards to the climate and therefore, is within the framework of other international agreements, like the Paris Agreement [2], [3].

One does not fulfill such targets with ease and therefore, several transformations are inevitable in industries around the world. The intensive research in renewable energy systems indicates the potential of renewable electricity for the efficient and carbon-free operation of such industries. Moreover, modes of transportation such as road and rail have been able to integrate with renewable energy systems such as wind and solar [4], [5]. However, this has not been the case for water and air transportation as they rely heavily on carbon based fuels. Therefore, carbon recycling can prove to be a potential solution in reducing $CO_2$ emissions.

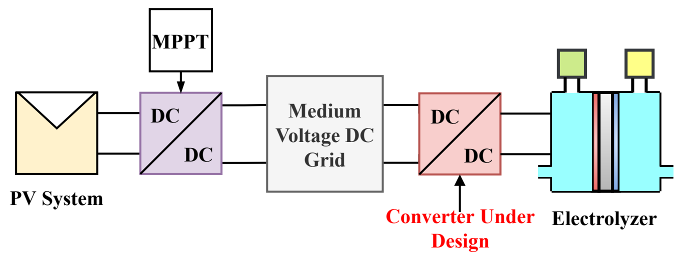


Fig. 1: Structure of the system.

The reduction in $CO_2$ can be achieved in two ways: thermo-chemical conversion into carbon based products and fuels and, $CO_2$ electrolysis. Power electronics based electrolysis systems has tremendous potential if energy dense fuels are produced with renewable electricity. Solutions up to the MW range in industries have been developed [6]. In [7], the challenges and future trends of low temperature electrolysis have been discussed. Here, study of various system architectures along with review of converter topologies for high power electrolysis has been carried out. According to their study, direct three-phase AC inverter is preferred for a grid-connected system, current-doubler secondary for parallel cell connection and, multi-port converter for independent connection architecture. The aim of this study is to introduce the concept of adaptive modularity in power electronics converter utilized for such applications. Electrolysis requires low voltage and very high current. If a single converter is utilized for this purpose, the converter efficiency will be very low. The focus therefore, should be to redistribute this current among several modules derived from a parent topology. Moreover, due to prolonged operation of the converter, the lifetime of the components, especially the semi-conductor switches starts to deteriorate. As a result, converter reliability starts to decrease. Therefore, the converter must intelligently be able to identify the operating point, and control the required modules such that the converter reliability is maintained and the efficiency is enhanced.
Fig. 1 provides the system structure for this study. The system specifications considered for future prototype development are shown in Table I. A Photovoltaic (PV) system is integrated with the medium voltage direct-current (MVDC) grid with

TABLE I: System specifications considered for future prototype development

| Parameter | Value |
|---|---|
| Input Voltage | 1.4 kV |
| Rated Power | 100 kW |
| Expected Stack Voltage | 70 V |

the help of a DC-DC converter operating on the principle of Maximum Power Point Tracking (MPPT). An additional DC-DC converter acts as a power electronics interface (PEI) between the MVDC grid and the electrolyzer. There are mainly 3 types of electrolyzers: Alkaline water, proton exchange membrane (PEM) and Solid Oxide Electrolyzers (SOEC). Alkaline electrolyzer technology is the most widely used and mature technology [8]–[10]. General Electric developed the first PEM electrolyzer based on the solid porous electrode concept in the 1960s [11]. This was based on the concept introduced by Thomas Grubb, where a solid sulfonated polystyrene membrane was used as an electrolyte [12], [13]. As the name suggests, the PEM electrolysis cell allows the transportation of protons from the anode to the cathode.

The process of solid oxide electrolysis was reported by Dönitz and Erdle as part of the HotElly project at Dornier System GmbH in the 1980s [14]. The RELHY project [15] targeted the development of novel or improved, low-cost materials (and the related manufacturing process) for SOECs. This research indicated that the materials developed could be operated at high temperature and could be used for the electrolysis of $CO_2$ to CO, and also the co-electrolysis of $H_2O/CO_2$ to $H_2$/CO (syngas).

The paper is organized as follows: Section II explains the modelling process for an alkaline electrolysis cell followed by it's modification to behave as a regenerative stack. Section III describes the converter design challenges, trade-offs and operational challenges. Section IV provides a review of the studied converter topologies in the literature. Section V explains the concept of adaptive modularity and how it can be applied for the considered configurations. Section VI provides conclusions and future work.

## II. Electrolysis Cell/Stack Modelling

To get a preliminary insight a pre-defined alkaline electrolyzer system will be utilized.

Several modelling approaches have been shown in literature [10], [16]–[18]. Despite some differences, every approach divides the cell modelling mainly into four steps. The approach followed in [17] will be applied for this study.

The voltage across an electrolysis cell is developed as a result of the contributions made by the following four potentials:

### A. Reversible Potential

The reversible potential of alkaline electrolysis cell exhibits thermodynamic effect. The reversible potential is given by the Nernst Equation:

$$V_{\mathrm{rev}} = V^0_{\mathrm{rev,T_k}} + \frac{RT_{\mathrm{k}}}{zF} \ln\left(\frac{(P - P_{\mathrm{KOH}}) \cdot \sqrt{P - P_{\mathrm{KOH}}}}{a_{\mathrm{H_2O,KOH}}}\right) \tag{1}$$

where, $V_{\mathrm{rev}}$ is defined as the reversible cell voltage, V. $V^0_{\mathrm{rev,T_k}}$ is defined as the temperature dependent reversible voltage, V. $R$ is known as the universal gas constant, $\mathrm{JK^{-1}mol^{-1}}$. $T_{\mathrm{k}}$ is the cell temperature, K. $P$ is the absolute pressure, bar. $z$ is defined as the number of moles of electrons transferred for 1 mol of product. $F$ is the Faraday constant, C $\mathrm{mol^{-1}}$. $P_{\mathrm{KOH}}$ is the vapour pressure of KOH, bar. $a_{\mathrm{H_2O,KOH}}$ is known as the water activity of KOH solution.

### B. Activation Potential

Activation potential refers to the interaction of electrolyte (chemical species) and electrodes via electrical charges. It refers to the double layer effect which is formed at the cathode of the cell [19]. In continuous DC operation, the activation phenomena is represented in the form of a non-linear voltage [20], [21]. However, the approach followed in [17] represents this as a parallel combination of a capacitor (electrode capacitance) and current-controlled voltage source for each electrodes.

The activation potential of both the electrodes can be represented by the modified Tafel Equations:

$$V_{\mathrm{act(ano)}} = s \ln\left(\frac{i_{\mathrm{act(ano)}}}{t} + 1\right) \tag{2}$$

$$V_{\mathrm{act(cat)}} = v \ln\left(\frac{i_{\mathrm{act(cat)}}}{w} + 1\right) \tag{3}$$

where, $s$, $t$, $v$, $w$ are temperature dependent constants. $i_{\mathrm{act(ano)}}$ and $i_{\mathrm{act(cat)}}$ are activation currents for anode and cathode respectively. The temperature dependent constants are determined with the help of curve-fitting and experimental data in contrast to the traditional exchange current density parameter due to the significant variation in the numerical values used in the literature [22]. Electrode's capacitance can be obtained by electro-chemical impedance spectroscopy (EIS), which is done by injecting a small-signal current perturbation at a wide range of frequencies and measuring the voltage [17].

### C. Ohmic Potential

Ohmic potential refers to the internal resistance offered by the electrolyte across the electrodes. This is represented by a temperature dependent resistance.

$$V_{\mathrm{ohm}} = i_{\mathrm{cell}} \cdot R_{\mathrm{ohm}} = i_{\mathrm{cell}} \frac{r}{A_{\mathrm{elect}}} \tag{4}$$

where, $r$ is the area-specific resistance of one of the electrolysis cells, ($\Omega\mathrm{m}^2$) and therefore, can be obtained from the experimental static current-voltage (I-V) characteristics at different temperatures of the electrolyzer with the help of curve-fitting techniques. $i_{\mathrm{cell}}$ is the cell current, A. $A_{\mathrm{elect}}$ is the electrode surface area, $\mathrm{m}^2$. $R_{\mathrm{ohm}}$ is the internal resistance of the electrolyzer cell, $\Omega$.

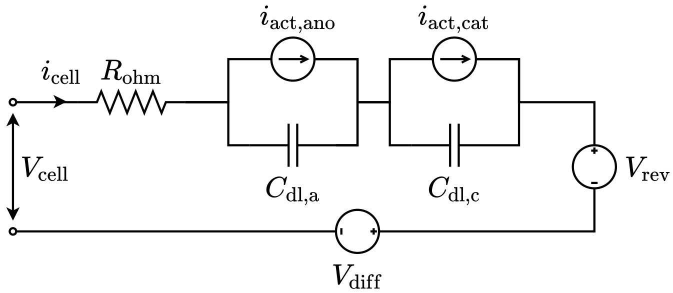


Fig. 2: Detailed equivalent circuit of the electrolysis cell.

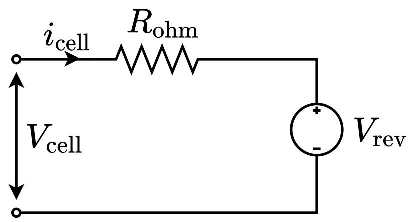


Fig. 3: Simplified equivalent circuit of the electrolysis cell.

### D. Diffusion Potential

Diaphragm or membranes utilized in electrolyzers are used to ensure that the products (gases/water molecules) obtained on both sides do not diffuse into each other. However, these components are not perfect, and therefore, when the process is carried out at high current and pressure, these products tend to diffuse into each other. This develops an over-potential that occurs due to the concentration difference between the two electrodes, and initiates diffusion. For instance, water molecules diffuse from anode to cathode through the polymer membrane in PEM electrolyzer [23], [24]. This diffusion leads to an inefficient operation. The electrolyzer which is to be modelled is an alkaline electrolyzer and hence, this contribution has not been considered.

### E. Cell Voltage

In case of the detailed model illustrated in Fig. 2, the cell voltage is given by,

$$V_{\text{cell}} = V_{\text{rev}} + V_{\text{ohm}} + V_{\text{act}} + V_{\text{diff}} \tag{5}$$

To simplify the modelling process, the activation potentials and the diffusion potentials have been neglected. As a result, the resulting equivalent circuit can be redrawn as shown in Fig. 3. The cell voltage can then be computed as follows:

$$V_{\text{cell}} = V_{\text{rev}} + V_{\text{ohm}} \tag{6}$$

This approach is extended for making a regenerative stack consisting of $N_{\text{s}}$ series-connected cells.

## III. Design Challenges and Trade-Offs

Characteristics shown in Fig. 4 do not give complete information about the behaviour of the regenerative stack. Therefore, it is important to study the effects of varying certain parameters of the regenerative stack on it's electrical characteristics. For this study, parameters considered are stack temperature, electrode surface area, number of series connected cells and molar concentration of the electrolyte. Table II summarises the potential converter design challenges and trade-offs for high power electrolysis based on the results of the sensitivity analysis of the alkaline regenerative stack.

### A. Operational Challenges

In Fig. 4 (B), the power rating of the stack during the fuel cell mode of operation is much smaller than the power rating during the electrolysis cell mode of operation resulting in an asymmetrical characteristics of the stack. This is because of the voltage drop across the internal resistance and current direction [28]. More importantly, the area that is bounded by these curves for a given temperature defines the operating region of the converter under design. The converter must be highly efficient over this wide operating region.

In addition to these challenges, the converter must be able to provide galvanic isolation in accordance to ISO2274:2020 standard for hydrogen generators using water electrolysis and ISO19880-1:2020 standard for gaseous hydrogen fueling stations makes it obligatory for the frames and enclosures to be grounded that become energized under first fault conditions. The transformer under design would have a large turns ratio and therefore, leakage inductance will be dominant. The switch selection must be carried out appropriately based on the maximum thermal handling capability which indirectly defines the current handling capability as conduction losses will be dominant on the stack side.

## IV. Converter Topology

DC-DC converters can be mainly classified on the basis of the ability to provide galvanic isolation [29]. It is necessary for this study to have an isolated DC-DC converter in accordance to standards discussed in the previous section. Therefore, review of isolated DC-DC converters will be carried out.

In [30] a DC-DC converter topology consisting of a full-bridge converter and a rectifier was proposed. The fuel cell is connected to the full-bridge converter which is interfaced with the rectification unit via a multi-winding transformer. The leakage inductance introduced in the circuit due to the inclusion of this transformer is utilized for incorporating Zero-Voltage-Switching (ZVS) in the full-bridge. The secondary side consists of multiple electro-mechanical relays that control the transformation ratio. The relay operation is stack voltage dependent. A 3 kW prototype was developed and an efficiency of 96.5 %. The transformer losses accounted for 50 % of the total losses at 1 kW and the losses in Metal Oxide Semi-Conductor Field Effect Transistors (MOSFET) accounting for 20 %. However, it should be noted that the rectification unit consists of diodes and therefore, power flow is unidirectional. Seoul National University of Technology proposed a design for integrating fuel cells with residential loads [31]. The design had 3 stages namely, front-end DC-DC converter, DC-AC

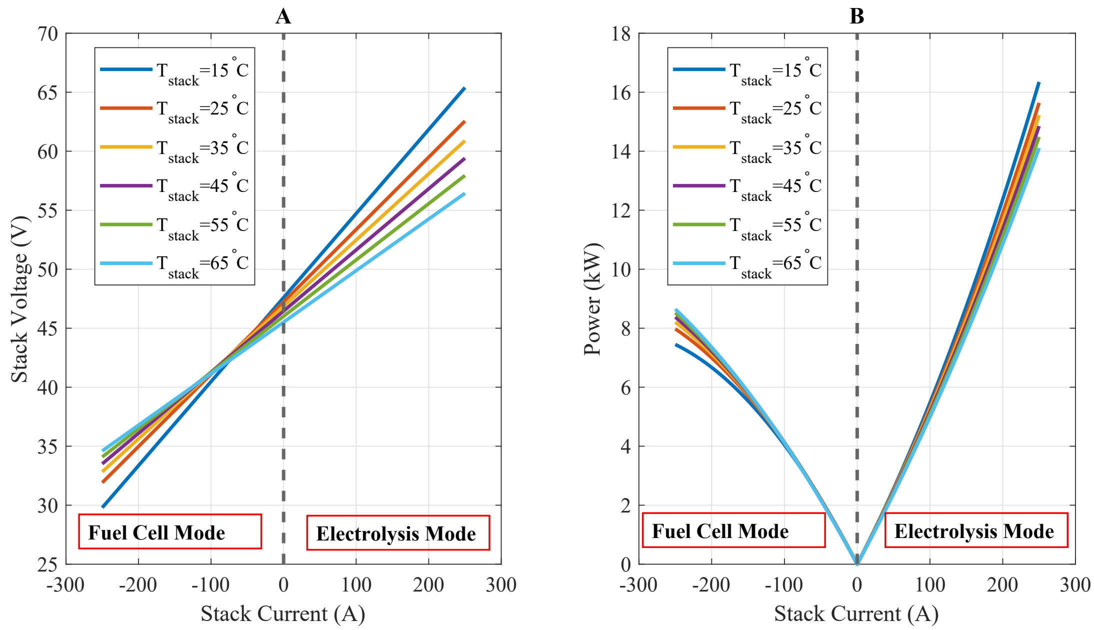


Fig. 4: Simplified Electrical Characteristics of the Regenerative Alkaline Stack, (A): Current-Voltage Characteristics; (B): Current-Power Characteristics.

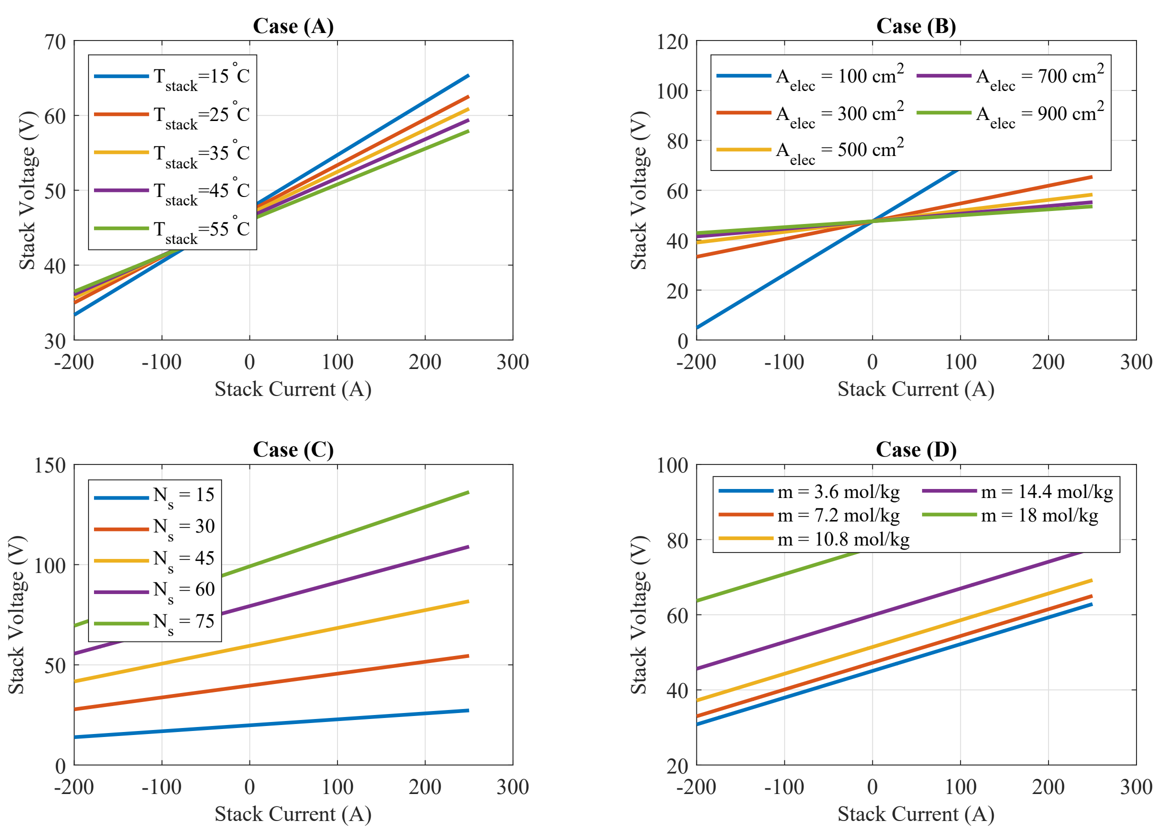


Fig. 5: Sensitivity analysis results for the considered alkaline regenerative stack, Case (A): Impact of stack temperature; Case (B): Impact of electrode surface area; Case (C): Impact of number of series connected cells; Case (D): Impact of molar concentration.

TABLE II: Converter Design Challenges, Preferences and Trade-Offs for High Power Electrolysis

| **Parameter** | **Effect on electrical characteristics** | **Preference from converter design perspective** | **Challenges/Trade-offs** |
|---|---|---|---|
| Stack temperature | Higher stack temperature increases ion mobility thereby, increasing the stack current. | Temperature of 15°C would be preferred to have a higher stack voltage for achieving a lower operating current for the given rated operating power to reduce the conduction losses in the converter | Thr hydrogen production rate reduces with decrease in stack temperature [25]. |
| Electrode Surface area | Influences the stack current in accordance to Cottrell's Equation [26]. Internal resistance is inversely proportional to the surface area and directly proportional to the distance between the two electrodes in accordance to Ohm's law. | Curve corresponding to $A_{\text{elec}}$ = 100 cm$^2$ would be preferred as it provides the highest possible stack voltage at a lower operating current for the same rated operating power. This implies lower losses in converter and stack as well as component derating in current magnitude. | A smaller electrode surface area strongly influences the internal resistance thereby, leading to higher losses in the electrolyzer. For $A_{\text{elec}}$= 100 cm$^2$, a boundary breach was detected where the internal resistance of the electrolyzer increased drastically. This is due to it's dependence on the distance between the electrodes as well as their surface area. |
| Number of series connected cells | Influences the reversible stack voltage as well as the internal resistance. | Higher number of series connected cells is preferred to achieve a higher stack voltage so that a lower operating current is achieved for the given rated operating power as this can lower converter current rating and lower losses. | Limitations are imposed on this parameter due to issues associated with equalizing fuel/gas pressure within the cells [27]. |
| Molar concentration of electrolyte | Influences the stack voltage and therefore, the internal resistance of the electrolyzer. | An electrolyte with higher molar concentration would be preferred to achieve a higher stack voltage so that a lower operating current is achieved for the given rated operating power. | Periodic purging of electrolyte is essential in an alkaline electrolyzer. This ensures that the molar concentration is maintained. The amount of electrolyte that can be injected into the system is defined by the reservoir capacity. This is desirable only at an industrial scale. In residential applications, water can be used as a substitute for an alkaline electrolyte and a cyclic process is achieved wherein hydrogen is generated, stored and utilized to produce electricity and water. However, in the case of water, the curves shown in Case C will be at a much lower stack voltage which is not desirable from the perspective of converter design. Moreover, increasing the molar concentration increases the viscosity of an electrolyte. This may result in higher electrical losses in circulating pumps as they have to do more work for the circulating this electrolyte. |

converter and an auxiliary power supply operated by a bi-directional DC-DC converter. Phase-shifted ZVS was utilized for this topology to minimize switching losses and the series connection of DC outputs allowed the reduction of transformer turns ratio. The reported efficiency was found to be 90 %. However, MOSFETs in high voltage (HV) bridge are required to carry the full load current and therefore, they need to have higher thermal handling capability. The transformers on the primary side are branched after the full-bridge and therefore, control over the branch currents is lost. As a result, this topology requires appropriate control such that power is evenly distributed among the transformers. More importantly, ZVS no longer is applicable at lighter loads and therefore, leads to high switching losses in the MOSFETs.

Virginia Tech [32] proposed a topology that consisted of 3 full-bridges on the primary side and 3 phase uncontrolled rectifier on the secondary side. A 3 phase transformer has been utilized for this design. Reported efficiency was 96 %. This topology does not suffer from the issue of operating at lighter loads in comparison to the topology discussed in [31]. Nevertheless, it has a similar problem of current distribution as discussed in [32] due to the series-parallel connection on the secondary side.

In [33], the proposed topology addresses the issues dis-

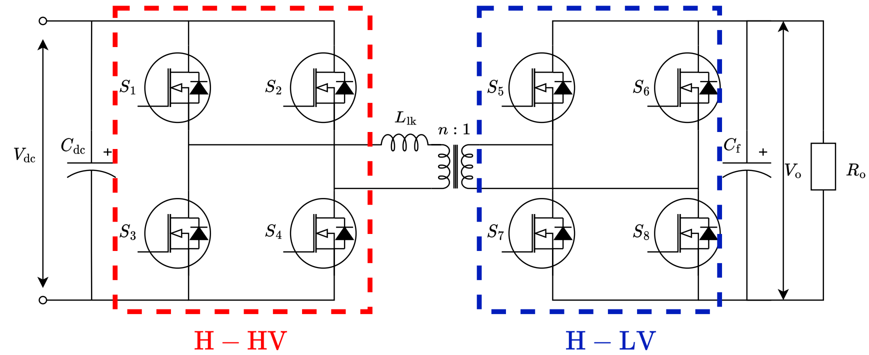


Fig. 6: Dual Active Bridge Converter.

cussed in [31], [32]. The transformers were center tapped, each accommodated with their own rectification unit and connected in series thereafter. The center tapping lead to reduction in turns ratio irrespective of the mode of operation. The series connection forced the current to be the same which in turn forces the primary side current to be the same. The even distribution of the current on the primary side allows the converter to operate at a higher efficiency despite being at light loads. This makes the converter behave as if it is operating at full load and ensure ZVS operation over the entire range. The reported efficiency was found to be 96.4 % at full load. [34] proposed a multi-port bidirectional system. The system consisted of CLLC resonant converter and an interleaved buck converter. The power flow in each parallel connected stack is controlled independently with the help of the interleaved buck converters. Each stack therefore, was decoupled. [35] proposed a Partial Parallel Dual Active Bridge Converter ($P^2$DAB) for high power renewable energy system integration. This topology offered 2 degrees of freedom to control either voltage or power. A similar connection as discussed in [33] has been utilized to force the current components on the low voltage (LV) side to remain essentially the same. Experimental results indicated that by regulating the phase angles, the converter efficiency can be improved at light loads. Based on this review, two parent topologies were identified, Dual Active Bridge (DAB) and resonant converter. For this study, the dual active bridge converter has been chosen due to it's ability to provide galvanic isolation, operate at a very high efficiency (greater than 99 %) and the ability to incorporate soft-switching without introducing additional passive components in contrast to the resonant topology.

## V. Concept of Adaptive Modularity

With reference to specifications provided in Table I, the stack current is expected to be,

$$I_{\text{stack}} = \frac{P_{\text{rated}}}{V_{\text{stack}}} = 1.42 \text{ kA}$$

This is extremely high current on the low voltage side of the converter. If a single converter was designed to deliver this current, the overall losses especially, the conduction losses will be dominant and converter efficiency would deteriorate. More

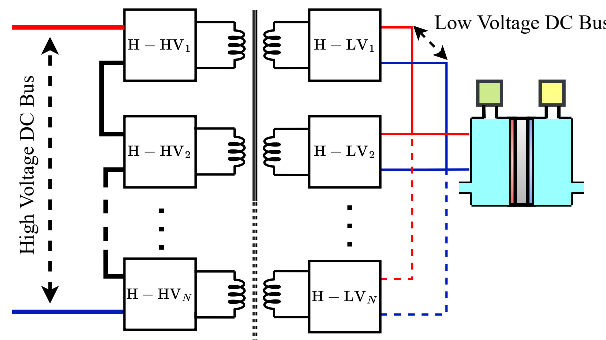


Fig. 7: Configuration A: Series connected H-HV and parallel connected L-LV bridges for a common electrolyzer stack.

importantly, due to prolonged operation, the switches on the low voltage side will have a smaller life-time and therefore, reliability takes a bigger hit. This is evident from the converter topology review discussed in the previous section.

Adopting a modular architecture for the converter utilized in such an application may prove to be potential solution to achieve this objective. [36] provides an overview of isolated dual active bridge converter for high frequency link power conversion systems. The authors have emphasized on the typical applications of DAB for high power link AC-AC Solid State Transformer (SST), DC-DC SST and Back to Back (BTB) configurations. In this paper, multiple DAB modules are used as power electronic interfaces between the DC grid and the electrolyzer stacks to handle the high operating current rating, each consisting of two H-bridges as shown in Fig. 6. Herein, H-HV and H-LV are the HV- and LV- side H-bridges respectively. Three different configurations are considered to redistribute the current on the LV side and ensure that there is minimal stress on the switches, and therefore improve efficiency of the system.

*1) Configuration A (Fig. 7):* Each DAB module is connected in series on the HV side and in parallel on the LV side. This may be beneficial as the voltage and current rating of individual switches for H-HV and H-LV bridges can be reduced by $\frac{1}{N}$, respectively. This is similar to topology proposed in [37] that describes DAB systems for MVDC

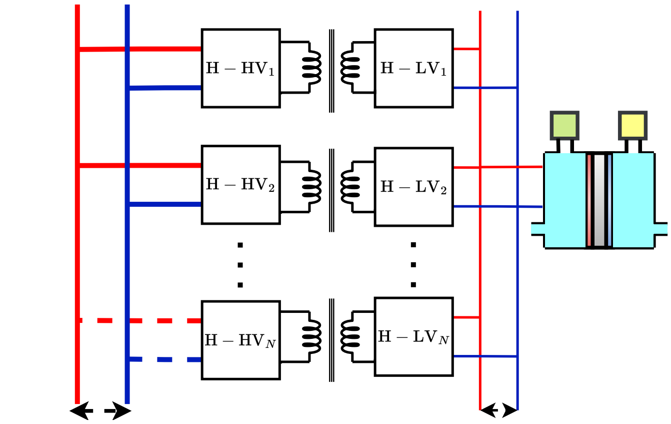

Fig. 8: Configuration B: Parallel connected H-HV and parallel connected H-LV bridges for a common electrolyzer stack.

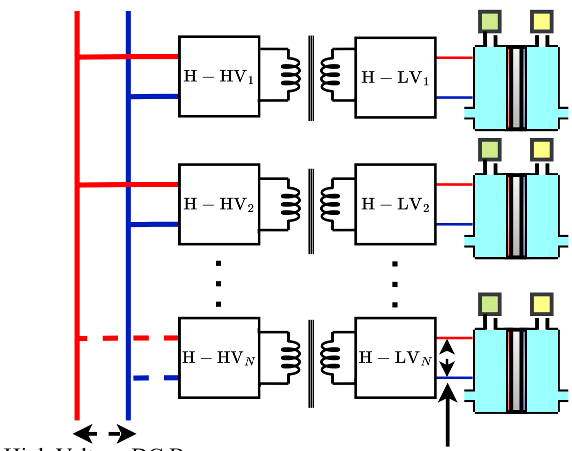

Fig. 9: Configuration C: Parallel connected H-HV and parallel connected H-LV bridges for a dedicated electrolyzer stack for each DAB module.

distribution grids.

*2) Configuration B (Fig. 8):* Each DAB module is connected in parallel to the DC bus on both the HV- and LV- side of the system. While the current rating of individual switches of the H-LV bridges reduces by $\frac{1}{N}$, the voltage rating of all H-HV bridge switches must be rated according the dc grid voltage. However, unlike configuration A, each DAB module can be activated or deactivated during operation to route the power efficiently between the electrolyzer and the grid.

*3) Configuration C (Fig. 9):* Each DAB module is connected to a dedicated electrolyzer stack such that there are N independent systems, each with power rating $\left(\frac{1}{N}\right)^{\text{th}}$ of the rated system power. Depending on the adaptive operation of DAB modules in accordance to the power flow, the IV-characteristics of the active stack can be modified, thus influencing the system efficiency.

## VI. Conclusions and Future Work

The presence of low voltage and high current at the stack side is not straight-forward to solve from the converter design perspective. This necessitates to develop power electronics solutions with the objective of redistributing this current such that the losses are minimized. In this paper, a simplified model of an alkaline regenerative stack is developed and the effect of varying certain parameters on it's electrical characteristics is discussed. Furthermore, the insights obtained from the same is co-related with the power electronics converter design challenges, operational challenges and their associated trade-offs with regards to the electrolyzer system. A converter topology review has been conducted followed by introducing the concept of adaptive modularity for power electronics converter employed for green hydrogen production. Three potential configurations based on the DAB converter are introduced and the advantages of applying adaptive modularity on these configurations have been discussed.

As part of the future work, real time simulations of the configurations discussed in this paper will be studied. A small-scale prototype of a DAB converter will be developed followed by it's integration with a real-time simulation system offered by OPAL-RT Technologies. The goal is to have one converter module physically connected to the simulation model consisting of the remaining modules with the help of power hardware in loop. This provides flexibility in scaling up the system when needed and also to evaluate it's performance. Furthermore, due to large number of components in the final system, a reliability assessment will be conducted for (N-1) contingencies.

## References

[1] M. van Economische Zaken en Klimaat, "Klimaatakkoord," Aug 2019.
[2] E. Commission, "Eu climate strategies and targets," 2020.
[3] U. Nations, "Paris agreement," 2016.
[4] A. Government, "Renewables take to the skies, rails and roads," 2019. [Online]. Available: https://arena.gov.au/blog/renewables-take-to-the-skies-rails-and-roads/
[5] U. N. University, "European trains go down renewable route," 2017. [Online]. Available: https://ourworld.unu.edu/en/european-trains-go-down-renewable-route
[6] McPhy, "Industrial hydrogen: a 20 mw project in the netherlands," 2020. [Online]. Available: https://mcphy.com/en/press-releases/industrial-hydrogen-a-20-mw-project-in-the-netherlands/
[7] C. Pascalau, T. B. Soeiro, N. H. van der Blij, and P. Bauer, "Electrical energy conversion for low temperature electrolysis-challenges and future trends," in *2021 IEEE 19th International Power Electronics and Motion Control Conference (PEMC)*. IEEE, 2021, pp. 349–356.
[8] N. R. Shriyan, "Modelling of pv-electrolyzer system for optimum operation," Master's thesis, Delft University of Technology, 2020.
[9] M. Carmo, D. L. Fritz, J. Mergel, and D. Stolten, "A comprehensive review on pem water electrolysis," *International journal of hydrogen energy*, vol. 38, no. 12, pp. 4901–4934, 2013.
[10] Ø. Ulleberg, "Modeling of advanced alkaline electrolyzers: a system simulation approach," *International journal of hydrogen energy*, vol. 28, no. 1, pp. 21–33, 2003.
[11] L. Nuttall, A. Fickett, and W. Titterington, "Hydrogen generation by solid polymer electrolyte water electrolysis," in *Hydrogen energy*. Springer, 1975, pp. 441–455.
[12] W. Grubb, "Batteries with solid ion exchange electrolytes: I. secondary cells employing metal electrodes," *Journal of the Electrochemical Society*, vol. 106, no. 4, p. 275, 1959.
[13] W. Grubb, "Ionic migration in ion-exchange membranes," *The Journal of Physical Chemistry*, vol. 63, no. 1, pp. 55–58, 1959.

[14] W. Dönitz and E. Erdle, "High-temperature electrolysis of water vapor—status of development and perspectives for application," *International Journal of Hydrogen Energy*, vol. 10, no. 5, pp. 291–295, 1985.
[15] E. Commission, "Innovative solid oxide electrolyser stacks for efficient and reliable hydrogen production," 2016. [Online]. Available: https://cordis.europa.eu/project/id/213009
[16] D. Falcão and A. Pinto, "A review on pem electrolyzer modelling: Guidelines for beginners," *Journal of Cleaner Production*, vol. 261, p. 121184, 2020.
[17] A. Ursúa and P. Sanchis, "Static-dynamic modelling of the electrical behaviour of a commercial advanced alkaline water electrolyser," *International journal of hydrogen energy*, vol. 37, no. 24, pp. 18 598–18 614, 2012.
[18] N. Gallandat, K. Romanowicz, and A. Züttel, "An analytical model for the electrolyser performance derived from materials parameters," *Journal of Power and Energy Engineering*, vol. 5, no. 10, pp. 34–49, 2017.
[19] D. Aikens, "Electrochemical methods, fundamentals and applications," 1983.
[20] J. Koponen, V. Ruuskanen, A. Kosonen, M. Niemelä, and J. Ahola, "Effect of converter topology on the specific energy consumption of alkaline water electrolyzers," *IEEE Transactions on Power Electronics*, vol. 34, no. 7, pp. 6171–6182, 2018.
[21] A. Kosonen, J. Koponen, V. Ruuskanen, M. Niemela, J. Ahola, J. Geisbusch, and P. Kreideweis, "Dynamic behavior emulation of alkaline electrolyzer by power-hardware-in-the-loop," in *2018 20th European Conference on Power Electronics and Applications (EPE'18 ECCE Europe)*. IEEE, 2018, pp. P–1.
[22] A. S. Tijani, M. A. Ghani, A. A. Rahim, I. K. Muritala, and F. A. B. Mazlan, "Electrochemical characteristics of (pem) electrolyzer under influence of charge transfer coefficient," *international journal of hydrogen energy*, vol. 44, no. 50, pp. 27 177–27 189, 2019.
[23] C. Rozain and P. Millet, "Electrochemical characterization of polymer electrolyte membrane water electrolysis cells," *Electrochimica Acta*, vol. 131, pp. 160–167, 2014.
[24] B. Endrodi, E. Kecsenovity, A. Samu, F. Darvas, R. Jones, V. Török, A. Danyi, and C. Janáky, "Multilayer electrolyzer stack converts carbon dioxide to gas products at high pressure with high efficiency," *ACS energy letters*, vol. 4, no. 7, pp. 1770–1777, 2019.
[25] J. C. Ganley, "High temperature and pressure alkaline electrolysis," *International journal of hydrogen energy*, vol. 34, no. 9, pp. 3604–3611, 2009.
[26] "Cottrell equation," https://en.wikipedia.org/wiki/Cottrell_equation, accessed: 2022-07-15.
[27] R. Pittini, Z. Zhang, and M. A. Andersen, "Isolated full bridge boost dc-dc converter designed for bidirectional operation of fuel cells/electrolyzer cells in grid-tie applications," in *2013 15th European Conference on Power Electronics and Applications (EPE)*. IEEE, 2013, pp. 1–10.
[28] A. Brisse, J. Schefold, C. Stoots, and J. O'Brien, "Electrolysis using fuel cell technology," in *Innovations in fuel cell technologies*. Royal Society of Chemistry, 2010, pp. 263–286.
[29] N. Mohan, T. M. Undeland, and W. P. Robbins, *Power electronics: converters, applications, and design*. John wiley & sons, 2003.
[30] L. Zubieta and G. Panza, "A wide input voltage and high efficiency dc-dc converter for fuel cell applications," in *Twentieth Annual IEEE Applied Power Electronics Conference and Exposition, 2005. APEC 2005.*, vol. 1. IEEE, 2005, pp. 85–89.
[31] S.-S. Lee, S.-W. Choi, and G.-W. Moon, "High-efficiency active-clamp forward converter with transient current build-up (tcb) zvs technique," *IEEE Transactions on Industrial Electronics*, vol. 54, no. 1, pp. 310–318, 2007.
[32] C. Liu, A. Johnson, and J.-S. Lai, "A novel three-phase high-power soft-switched dc/dc converter for low-voltage fuel cell applications," *IEEE Transactions on Industry Applications*, vol. 41, no. 6, pp. 1691–1697, 2005.
[33] K. Sternberg and H. Gao, "A new dc/dc converter for solid oxide fuel cell powered residential systems," in *2008 34th Annual Conference of IEEE Industrial Electronics*. IEEE, 2008, pp. 2273–2277.
[34] X. Lin, K. Sun, J. Lin, Z. Zhang, and W. Kong, "A multi-port bidirectional power conversion system for reversible solid oxide fuel cell applications," in *2018 International Power Electronics Conference (IPEC-Niigata 2018-ECCE Asia)*. IEEE, 2018, pp. 3460–3465.
[35] Z. Zhang, K. Tomas-Manez, Y. Xiao, and M. A. Andersen, "High voltage gain dual active bridge converter with an extended operation range for renewable energy systems," in *2018 IEEE Applied Power Electronics Conference and Exposition (APEC)*. IEEE, 2018, pp. 1865–1870.
[36] B. Zhao, Q. Song, W. Liu, and Y. Sun, "Overview of dual-active-bridge isolated bidirectional dc–dc converter for high-frequency-link power-conversion system," *IEEE Transactions on power electronics*, vol. 29, no. 8, pp. 4091–4106, 2013.
[37] M. Stieneker and R. W. De Doncker, "Dual-active bridge dc-dc converter systems for medium-voltage dc distribution grids," in *2015 IEEE 13th Brazilian Power Electronics Conference and 1st Southern Power Electronics Conference (COBEP/SPEC)*. IEEE, 2015, pp. 1–6.